JOURNAL OF MATERIALS SCIENCE **34** (1999) 5361–5369

Pyroelectric and dielectric bolometer properties of Sr modified $BaTiO_3$ ceramics

J. H. YOO, W. GAO
Department of Chemical and Materials Engineering, The University of Auckland, New Zealand
E-mail: w.gao@auckland.ac.nz

K. H. YOON
Department of Ceramic Engineering, Yonsei University, Korea

The pyroelectric and dielectric bolometer properties of Sr modified $BaTiO_3$ ceramics were investigated for thermal IR detector applications. The $(Ba_{1-x}, Sr_x)TiO_3$ solid solution ceramics have been prepared by adding 10–40 at % $SrTiO_3$ to $BaTiO_3$ and with different sintering conditions and under dc fields. The relationships of processing parameters, microstructures, dielectric/pyroelectric properties and dc fields are discussed. And the "figures of merit" are compared between pyroelectric-type and dielectric bolometer-type IR sensors based on the experimental results.

1. Introduction

High performance and inexpensive infrared sensors are required for various applications at near ambient temperature such as thermal detection and object imaging. There are two modes for infrared detection. The first one is the conventional pyroelectric mode of IR detection, utilising the falling spontaneous polarisation. Above the phase transition, however, there is no spontaneous polarisation and hence no pyroelectric effect. This mode operates at a temperature sufficiently below the ferroelectric phase transition point to avoid inadvertent depoling that may occur by exceeding Curie temperature. However, the maximum pyroelectric effect occurs near the Curie temperature, and therefore it seems desirable to operate over a temperature range near the Curie point. So there has been considerable interest in using ferroelectrics close to their curie temperatures and under an applied bias. This led to the development of the second mode of pyroelectrics—dielectric bolometer. It is possible to operate at or above Curie temperature, with an applied bias field, in the mode of a dielectric bolometer. The effect of the applied electric field on the dielectric constant in the region of Curie temperature is both to reduce the magnitude of the dielectric constant, and to flatten and shift the dielectric peak [1]. Because dipoles depend on the voltage for sustaining dipole direction, an applied dc field adds an induced polarisation to the spontaneous polarisation and stabilises polarisation near the Curie temperature. Most of pyroelectric effect occurs when the materials have a perovskite structure. The non-centrosymmetrical crystal structure provides an asymmetric environment experienced by electrically charged species within a unique axis along which spontaneous polarisation exists. Their high polarisability yields large spontaneous polarisation and high dielectric permittivity [2]. As reported [3, 4], high polarisation is desirable since it often facilitates a substantial change with temperature, particularly at near Curie temperature. A high dielectric constant is also useful in many imaging applications because it controls the impedance matching of the target element to the read-out amplifier. As for the pyroelectric and dielectric bolometer mode applications, the family of ferroelectric materials that have the best properties is perovskite ceramics.

In this paper, the effects of mole fraction of $SrTiO_3$, sintering time and applied dc fields on the electric properties of $(Ba_{1-x}Sr_x)TiO_3$ system have been studied. The "figures of merit" for application of IR thermal sensors were calculated.

2. Experimental

The compositions of $(Ba_{1-x}Sr_x)TiO_2$ ceramics with $x = 0.1$, 0.2, 0.3 and 0.4 are named as BST10, BST20, BST30 and BST40, respectively. Regent grade $BaCO_3$, $SrCO_3$ and TiO_2 were used as starting materials to prepare these specimens. The respectively weighed powders were blended and calcined at 1000 °C for 10 h. The calcined aggregates were again wet milled and cold iso-pressed into disc-shaped samples at a pressure of 200 MPa. The disks were then sintered at 1350 °C for 2, 4, 6, 8 and 10 h in air. After sintering, the samples were cut from the sintered cylinders and polished down to a 1 μm finish and etched. The diameters and thickness of samples were about 1.0 and 0.3 mm, respectively. The surfaces were then silver electroded and poled by applying a dc field of 20 kV/cm over temperatures ranging from 30 to 80 °C in a silicone oil bath for 30 min.

2.1. Microstructural characterisation

The lattice parameters and average grain size were determined by X-ray diffraction (XRD) and scanning electron microscopy (SEM), respectively. The theoretical density and the tetragonality, which was defined as the ratio of the lattice constants c/a, were calculated from the least-square unit cell parameters. The apparent density was obtained following standard ASTM C373-72.

2.2. Electrical characterisation

The dielectric constants (ε_r) and dielectric loss tangents ($\tan\delta$) with dc bias ranging from 0 to 2.0 kV/cm were measured using an impedance analyser (Hewlett-Packard 4194A) at 1 kHz frequency between -20 and 120 °C. The pyroelectric coefficients (p_i) under 0 bias and dc field were determined by using the Byer and Roundy technique [5] in the temperature range of -20 to 120 °C. This technique employs a constant temperature increase dT/dt, and the output current is proportional to the pyroelectric coefficients. P-E hysteresis loops were determined with a modified Sawyer-Tower circuit. The dc-discharging current was measured using a Keithley 485 pA-meter as the temperature varied at a rate of 4 K/min. The temperature variation of specific heat (C_p) was measured with a PL-DSC system.

3. Results and discussion

XRD results indicate that each sample has a shifted perovskite structure as shown in Figs 1 and 2. The reflection line splitting is caused by a tetragonal distortion from the cubic perovskite cell. With the addition of $SrTiO_3$, the peak splitting was seen to decrease. The peaks were also moved to the high angle direction with increasing addition of $SrTiO_3$ and sintering time. This result indicated that the size of unit cell was decreased with increasing $SrTiO_3$. And with the increasing sintering time, the diffraction angle were slightly increased except for the specimens with 10 h sintering. These results indicated that the size of unit cell is dependent on the amount of $SrTiO_3$ rather than the sintering time. The tetragonality (c/a) decreased with increasing addition of $SrTiO_3$ and sintering time as shown in Table I. These results could be explained by the sinterability and the effect of the ionic size difference between Ba^{2+} and Sr^{2+}. The $BaTiO_3$ has a structure of loosely packed oxygen octahedra due to the presence of large Ba^{2+} ions in the perovskite lattice. When the Ba^{2+} ions are substituted with isovalent ions of smaller size, such as Sr^{2+}, the adjacent oxygen will displace toward the substituents to have a more closely packed structure.

TABLE I Tetragonality (c/a) of $Ba_{1-x}Sr_xTiO_3$ specimens with various sintering time

	Time (h)				
Composition	2	4	6	8	10
BST10	1.0069	1.0065	1.0060	1.0026	1.0089
BST20	1.0056	1.0041	1.0036	1.0017	1.0061
BST30	1.0042	1.0033	1.0027	1.0009	1.0047

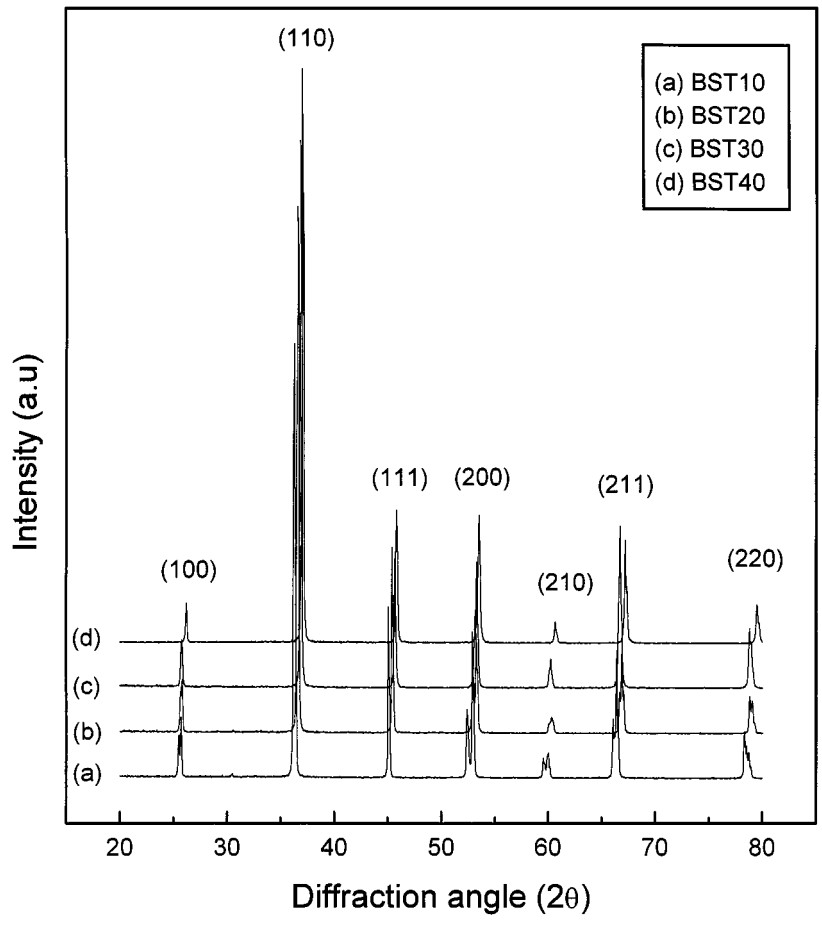

Figure 1 X-ray diffraction patterns of $Ba_{1-x}Sr_xTiO_3$ sintered at 1350 °C for 2 h: (a) BST10, (b) BST20, (c) BST30, and (d) BST40.

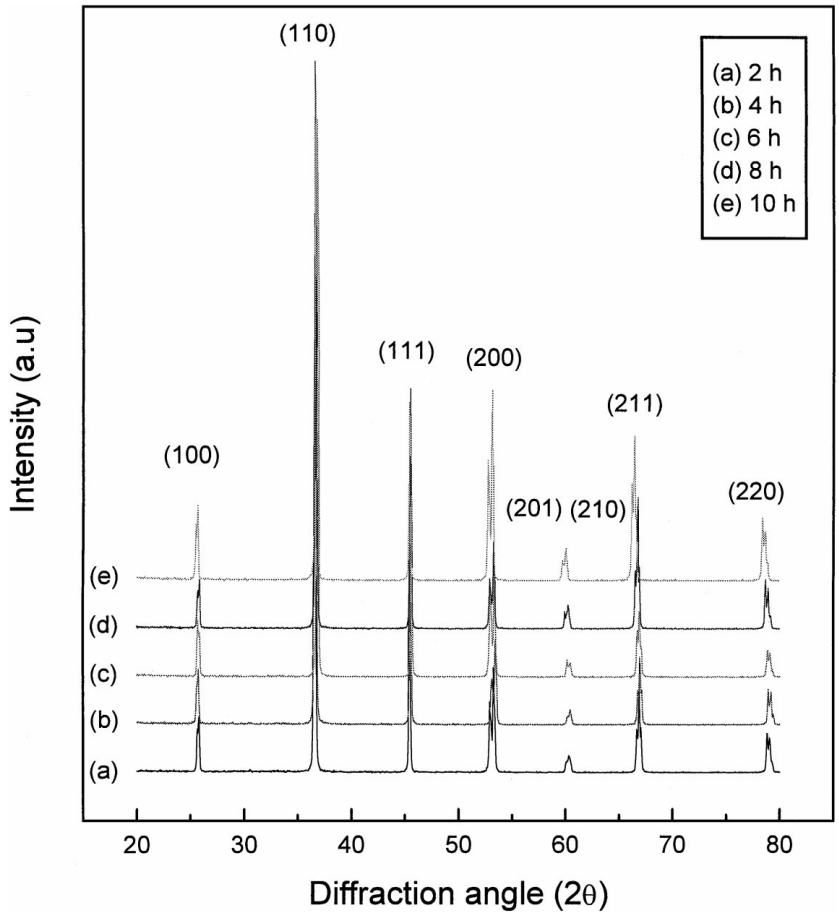

Figure 2 X-ray diffraction patterns for BST20 compounds sintered at 1350 °C for: (a) 2 h, (b) 4 h, (c) 6 h, (d) 8 h, and (e) 10 h.

SEM analysis for BST specimens revealed that the grain size decreases with increasing $SrTiO_3$ additions and increases with sintering time, as shown in Figs 3 and 4. Abnormal grain growth took place and the distribution of grain size was showed bimodal distribution. With the increasing sintering time, the bimodal distribution was changed to the normal distribution. So grains became more uniform with increasing sintering time. However, in case of further sintering to 10 h, the number of large grains was reduced. This may be caused by the vaporisation of Ba during long time sintering (10 h). With the addition of $SrTiO_3$, the grain size decreased. The rate of nucleation and the rate of grain growth generally have opposite effect. The final grain size is influenced by the relative values of the rate of nucleation N and the rate of growth G. If the ratio of N to G is large, the final grain size will be small. Both rates strongly depend on processing parameters such as the composition and temperature [6, 7]. So the addition of $SrTiO_3$ caused a high nucleation rate with consequent early impingement of abnormal grain growth. Therefore sintering time and the mole fraction of $SrTiO_3$ are important factors for control the grain size and grain size distribution. During the grain growth, the pores were captured and the pore size at the grain boundaries were increased. With the increasing sintering time, the number of pores decreases but the size increases. The colour of sintered samples was yellow except light blue for the specimens after 10 h sintering. The average grain size was in the range of 10–35 μm.

The apparent and relative density increased with sintering time up to 8 h, and the maximum value of apparent density was 5.76 to 5.55 (g/cm^3). With sintering time, the variation of relative density was similar to the variation of uniformity of the grain size. Therefore density depends on the uniformity of grain size.

3.1. Dielectric properties

Fig. 5 shows the variation of the maximum dielectric constants (ε_r) at Curie temperature (T_C) for BST specimens as a function of the addition of $SrTiO_3$ in mol %. It can be seen that ε_r at T_C increased up to 30 mol % $SrTiO_3$ and then decreased. It is interesting that the low-temperature Curie point materials do not show the decrease in dielectric constant [8]. These results are consistent with Nomuro's, that a minimum activation energy obtained from dc measurements was found at 40% $SrTiO_3$ [8]. The Curie temperature decreased with the substitution of Sr^{2+} for Ba^{2+}. Thermal hysteresis was also examined and it was found that a 3 K delay exist for the maximum dielectric constant between heating and cooling. The Curie temperature obtained from DSC results was in agreement with the corresponding values determined from the dielectric and pyroelectric measurements. The Curie temperature was decreased slightly with increasing sintering time. The dielectric loss (tan δ) of BST samples had relatively low changes versus the composition and sintering time. It was in the range of 0.003–0.005. The dielectric loss increased to about 0.05 after 10 h sintering.

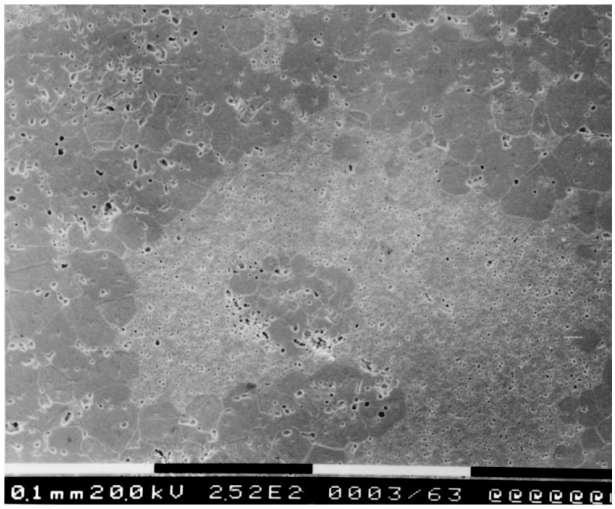

(a)

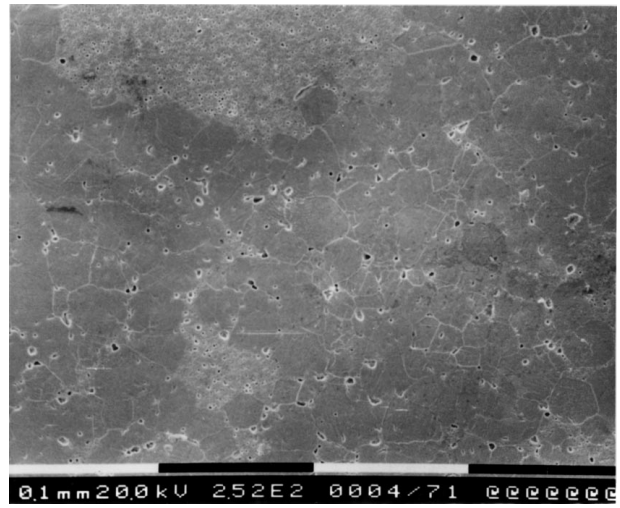

(b)

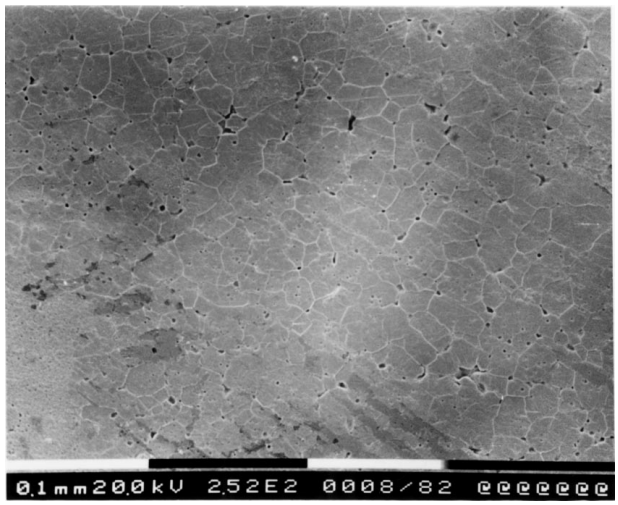

(c)

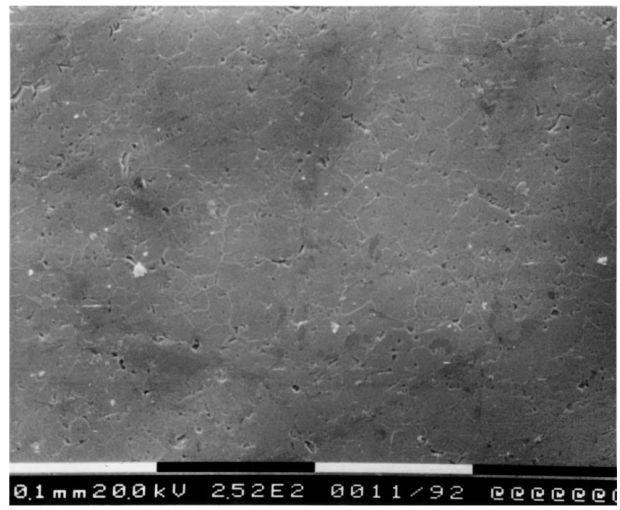

(d)

(e)

Figure 3 SEM image of microstructure for BST30 sintered at 1350 °C for: (a) 2 h, (b) 4 h, (c) 6 h, (d) 8 h, and (e) 10 h.

In BST30 specimens under a dc field, ε_r at T_C decreased with increasing field as shown in Fig. 6. With the applied voltage, the phase transition temperature was increased and the peaks were suppressed and broadened. It can be interpreted by considering the coexistence of the ferroelectric and paraelectric phases in the temperature range of diffusion phase transition [9]. The diffusion phase transitions in BST ceramics under dc fields may be explained in terms of a stress-induced coexistence of cubic, tetragonal, orthorhombic

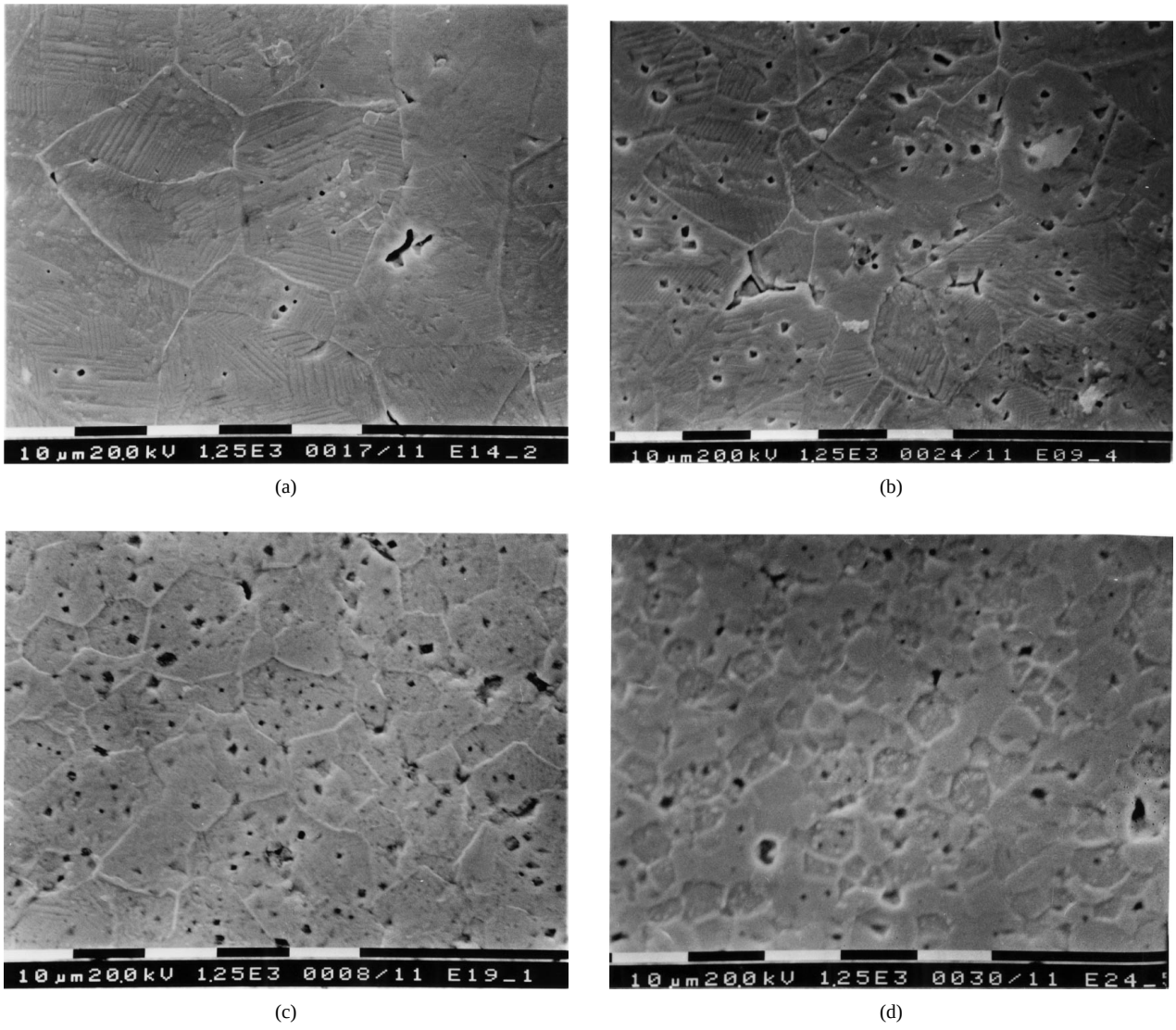

Figure 4 SEM image of microstructure for $Ba_{1-x}Sr_xTiO_3$ sintered at 1350 °C for 8 h: (a) BST10, (b) BST20, (c) BST30, and (d) BST40.

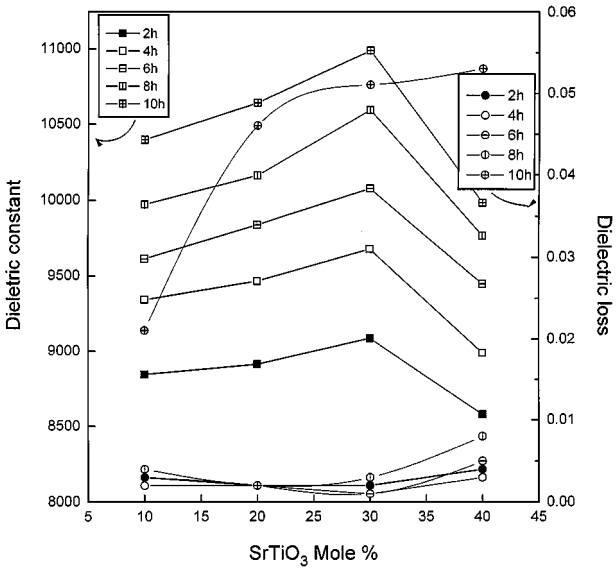

Figure 5 Dielectric constant and tangent of loss angle versus mol % of $SrTiO_3$ at T_C.

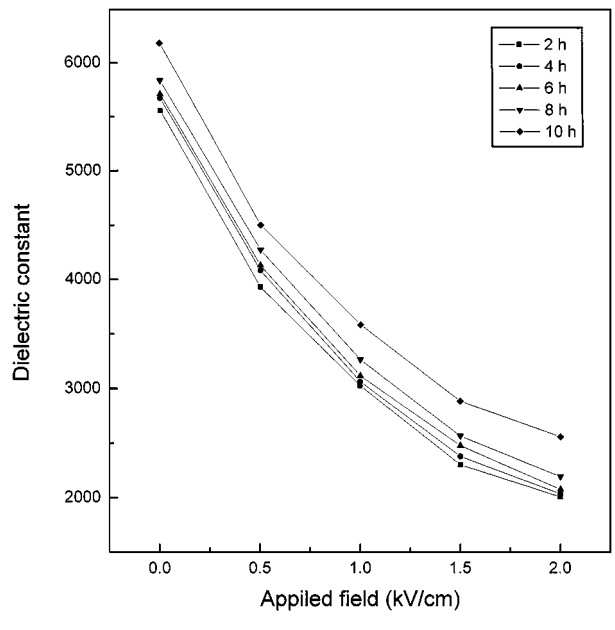

Figure 6 Dielectric constant versus applied field for various sintering time at room temperature for BST30 specimens.

and rhombohedral perovskite phases. Dielectric loss was less than 0.001, and it was also slightly suppressed with increasing field.

3.2. Pyroelectric properties

The variations of spontaneous polarisation (P_s) as a function of temperature of each of samples are shown in Fig. 7. The values of P_s were decreased with addition of $SrTiO_3$ and increased with sintering time except 10 h sintering, but did not vanish at Curie temperature. By using the Byer and Roundy technique [6], the pyroelectric current was measured in the temperature range of −20–120 °C. This technique is using a constant temperature ramp dT/dt and the output current is proportional to pyroelectric coefficient p_i. The main source of error with this measurement technique is the deviation from linearity in the temperature ramp. In this measurement, the maximum deviation is 0.05 K for the ramps of 4 °C/min. The variation of pyroelectric coefficients (p_i) for BST specimens as a function of the increasing $SrTiO_3$ added and sintering time are shown in Fig. 8. The p_i increased with increasing additions of $SrTiO_3$ up to BST30, and then to decrease in BST40. The sintering time also has a strong effect. The maximum p_i value is obtained after 8 h sintering. The specimen with the maximum pyroelectric coefficient corresponds to the composition with the minimum tetragonality (c/a) ratio and normal grain size distribution. As the grain size distribution becomes normal grain distribution, the number of domains increases and the spontaneous polarisation also increases, as shown in Fig. 7.

In BST30 composites sintered under a dc field, the dependence of induced p_i on the sintering time and field are shown in Table II. The value of p_i increased with increasing applied field. The maximum p_i was 6.02×10^{-6} C/cm^2 after 8 h sintering at 2.0 kV/cm. These results indicated that with decreasing tetragonality, the anisotropic of the unit cell decreases. Therefore, the 90° domains can reorient more easily with the applied field. Thus the samples treated with applied fields are more efficient in obtaining high pyroelectric coefficients. Because dipoles depend on the voltage for sustaining dipole direction, applied dc field adds an induced polarisation to the spontaneous polarisation and stabilises polarisation near T_C.

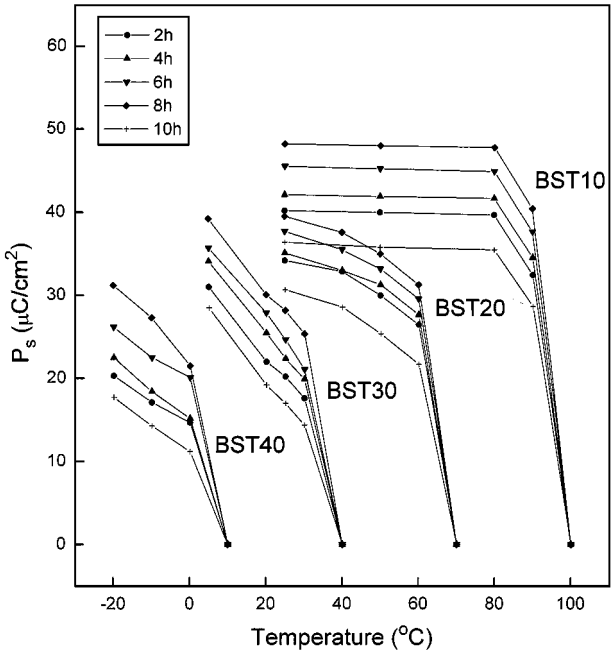

Figure 7 The variation of spontaneous polarisation with temperature in BST specimens.

TABLE II Pyroelectric coefficients (nC/cm^2 K) of BST30 under dc field

	dc (kV/cm)				
Time (h)	0	0.5	1	1.5	2
2	386.5	587.6	668.7	885.4	1826.2
4	426.7	765.2	1200.3	1742.6	2531.7
6	495.9	970.3	1954.5	2591.7	3777.4
8	675.6	1232.8	2504.5	4046.1	6017.8
10	322.2	859.6	1015.8	1697.6	2092.6

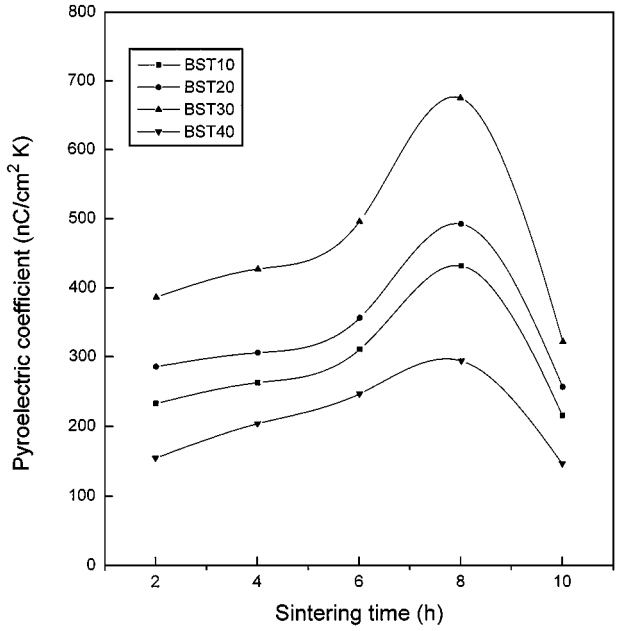

Figure 8 Pyroelectric coefficients versus mol % $SrTiO_3$ at T_C.

3.3. Pyroelectric characteristics of BST compounds

It is convenient to define an appropriate "figure of merit" for the particular application of interest [10]. Three of these figures were defined, calculated as follows:

$$F_i = \frac{p_i}{\rho C_p} \quad (1)$$

$$F_v = \frac{p_i}{\rho C_p \varepsilon_r} \quad (2)$$

$$F_d = \frac{p_i}{\rho C_p \sqrt{\tan \delta \varepsilon_r}} \quad (3)$$

These figures can serve as a guide in evaluating pyroelectric materials because the other factors are related to the operation conditions such as wavelength,

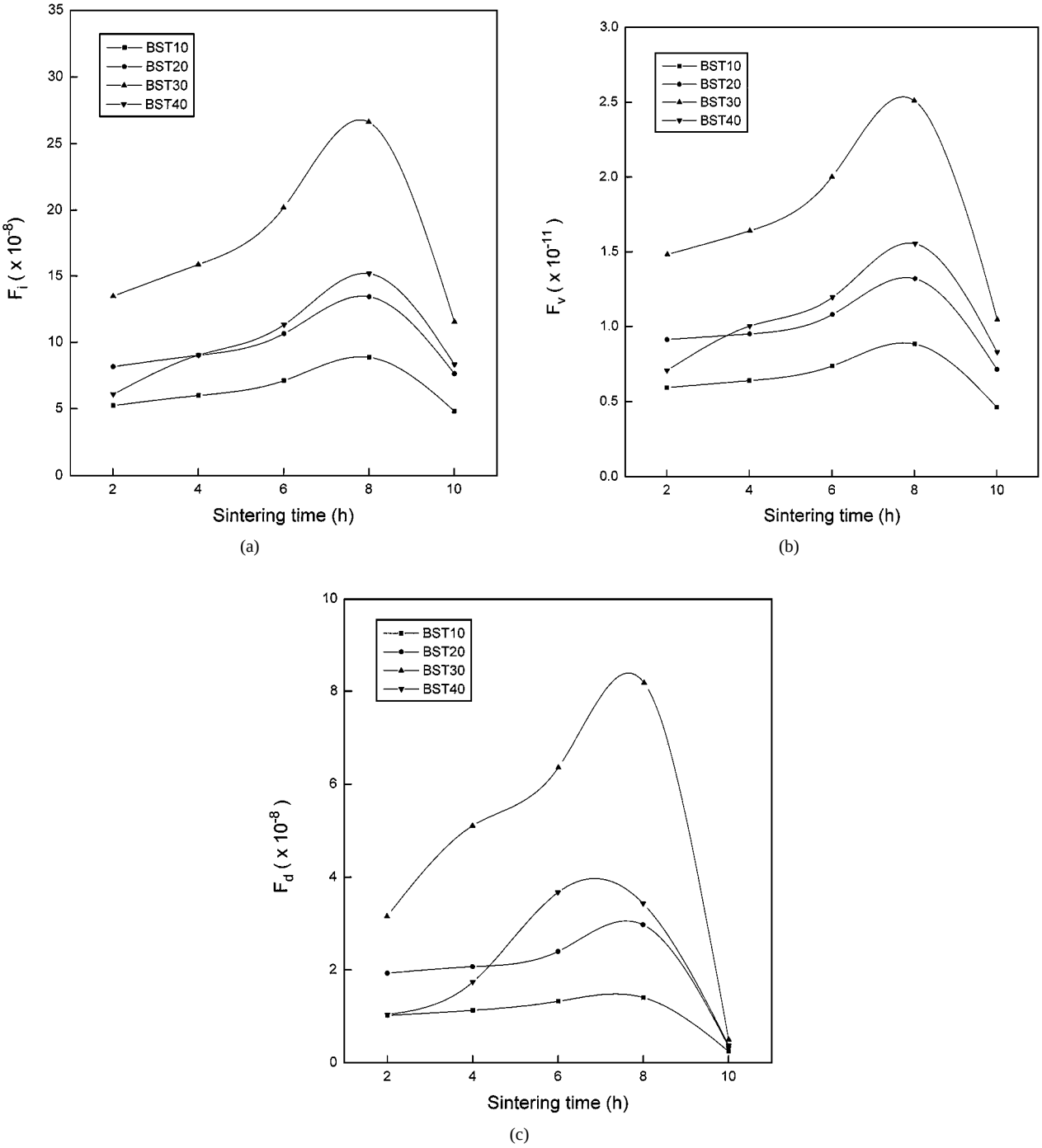

Figure 9 The variation of "figures of merit" with sintering time for $Ba_{1-x}Sr_xTiO_3$ specimens: (a) F_i, (b) F_v, and (c) F_d.

frequency band and amplifier parameters. The effects of $SrTiO_3$ additions in BST and the sintering time on these "figures of merit" were calculated and presented in Fig. 9. As shown in these figures, the estimated values of the "figures of merit" decreased after sintering for 10 h. The value of F_d decreased stiffly after sintering 10 h, due to the increasing dielectric loss. The values of the "figures of merit" increased as the addition of $SrCO_3$ increased, however there was a decreasing in the BST40 composites. In spite of the low pyroelectric coefficients, the "figures of merit" values of BST40 are slightly better compared to BST10 and BST20 composites. The reasons for these relatively high values for the BST40 composites are that they have a lower density and heat capacity. These results indicate that sintering time has very strong effects on the "figures of merit".

The "figures of merit" for BST30 under dc fields was also calculated and shown in Fig. 10. The values of the "figures of merit" were increased and broadened slightly as the applied voltage increased, reaching a maximum value after 8 h of sintering. The values of the "figures of merit" increased with sintering time up to 8 h, and then decreased after 10 h of sintering because there was a contribution to the tangent loss from the domain wall movement. That was caused by the increases of tangent loss after 10 h sintering. Contrary to the case with zero applied voltage, the peak values of the "figures-of merit" with various applied voltages increased with increasing applied voltage. This is

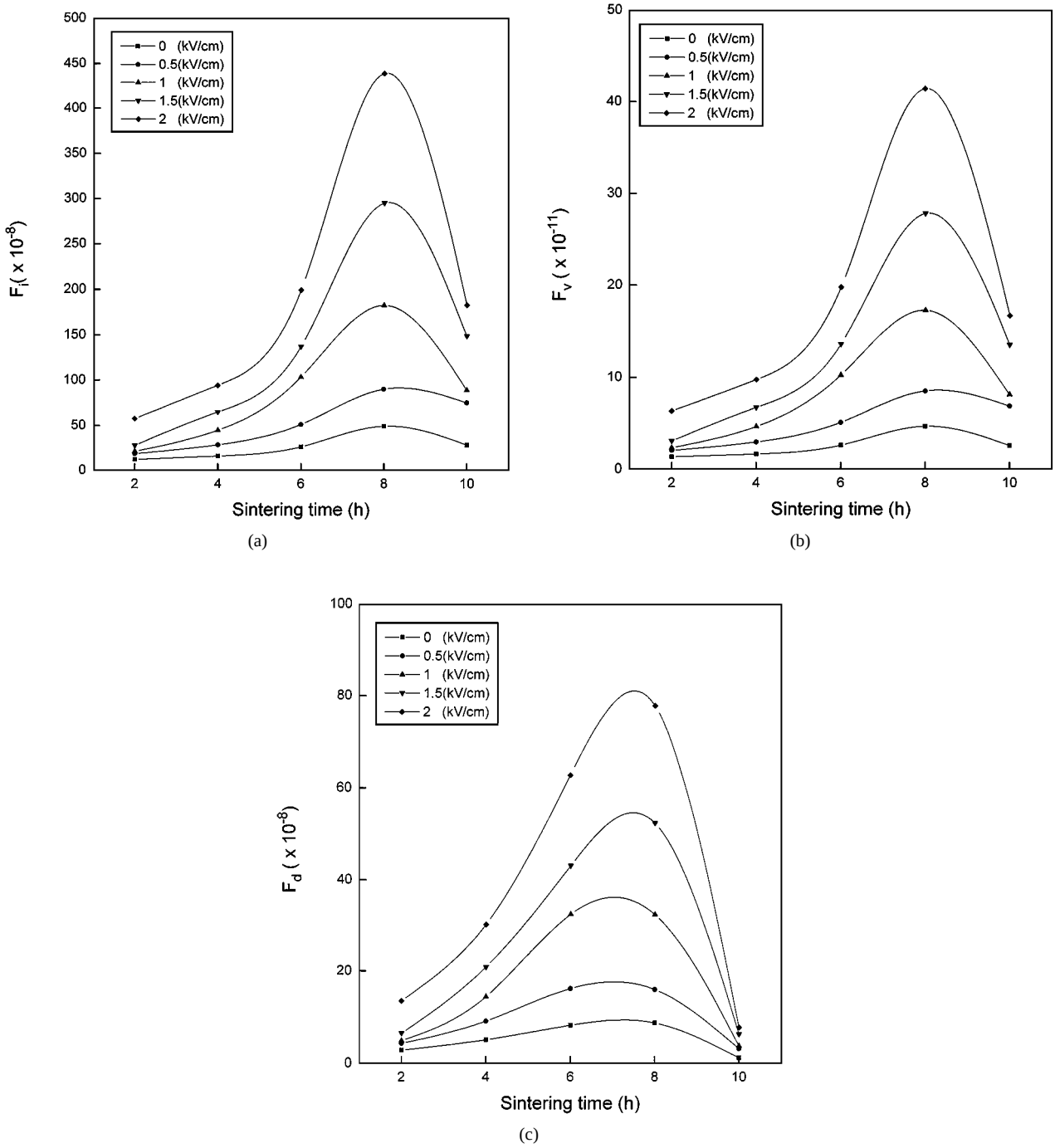

Figure 10 The variation of "figures of merit" with sintering time under dc field for BST30 specimens: (a) F_i, (b) F_v, and (c) F_d.

caused by the fact that both the dielectric constant and the dielectric loss decreased with increasing applied voltage. Furthermore, the peak value of the pyroelectric coefficient is strongly influenced by the applied voltage.

4. Conclusion

The dielectric and pyroelectric properties of BST compounds depend on the addition of $SrTiO_3$ and sintering time. The presented results suggested that BST30 compound with 8 h sintering at 1350 °C produces the best pyroelectric coefficient. Applied dc fields improved the properties of BST compounds by a factor of 10. The most practically significant result from this study is that the maximum pyroelectric coefficient corresponds to the uniform grain size and minimum *c/a* ratio.

Acknowledgements

The authors would like to thank Auckland University Research Council for partial support, and Professor D. H. Kang in Suwon University for assistance.

References

1. C. HANSON, H. BERATAN and S. MCKENNEY, *Proc. SPIE-Int. Soc. Opt. Eng., 1735 Infrared Detector* (1992) 17.
2. R. W. WHATMORE, *Ferroelectrics* **76** (1987) 351.
3. M. DAGLISH and A. J. MOULSON, *ibid.* **126** (1992) 215.

4. R. WATTON, *ibid*. **91** (1989) 87.
5. R. L. BYER and C. B. ROUNDY, *J. Appl. Phys*. **44** (1973) 929.
6. D. HENNINGS, *Int. J. High Technology Ceramics* **3** (1987) 91.
7. D. KOLAR, "Ceramic Transactions Vol. 7" (The American Ceramic Society, Columbus, Ohio, 1990) p. 529.
8. S. NOMURO and S. SAWADA, *J. Phys. Soc. Japan* **5** (1950) 227.
9. D. HENNINGS and A. SCHNELL, *J. Amer. Ceram. Soc*. **11** (1982) 539.
10. R. W. WHATMORE, *Rep. Prog. Phys*. **49** (1986) 1335.

Received 21 November 1997
and accepted 23 March 1999